ChemComm

Site-selective stepwise reduction of a corannulene-based chiral molecular nanographene with Na metal

Journal:	*ChemComm*
Manuscript ID	CC-COM-02-2022-000971.R1
Article Type:	Communication

COMMUNICATION

Stepwise reduction of a corannulene-based helical molecular nanographene with Na metal

Received 00th January 20xx,
Accepted 00th January 20xx

DOI: 10.1039/x0xx00000x

Zheng Zhou,[a,b] Yikun Zhu,[a] Jesús M. Fernández-García,[c] Zheng Wei,[a] Israel Fernández,*[c] Marina A. Petrukhina,*[a] Nazario Martín*[c,d]

The chemical reduction of a corannulene-based molecular nanographene, $C_{76}H_{64}$ (1), with Na metal in the presence of 18-crown-6 afforded the doubly-reduced state of 1. This reduction provokes a distortion of the helicene core and has a significant impact on the aromaticity of the system.

The discovery of fullerenes by H. Kroto, R. Curl and R. E. Smalley in 1985 and the vast array of new properties and applications developed with these spherical carbon nanostructures (buckyballs) opened up a new era in materials science.[1] Following this seminal discovery, bowl-shaped polycyclic aromatic hydrocarbons (PAHs) received special attention as formal fullerene fragments (buckybowls)[2] and, in turn, as suitable building blocks for the long-awaited synthesis of these new allotropic forms of carbon.[3] The founded carbon-based materials science reached a further landmark in 2004 with the discovery of graphene as a new carbon nanostructure by A. K. Geim and K. S. Novoselov.[4] Despite the outstanding chemical and physical properties of graphene,[5] its use as a semiconductor is prevented by the zero bandgap between its conduction and valence bands.[6]

Among the different procedures to open a bandgap for electronic applications,[7] quantum confinement of the electrons in small flakes of graphene,[8] the so-called nanographenes (NGs)[9] or graphene quantum dots (GQD),[10] has been extensively used. The controlled bottom-up preparation of monodisperse molecular NGs by organic chemistry protocols, offers new synthetic opportunities for PAHs as starting building blocks.[11] In particular, curved PAHs allow the construction of NGs endowed with Gaussian curvature. In this way, along the last recent years, a wide variety of curved nanographenes have been synthesized, including positively curved (bowl-shaped) or/and negatively curved (saddle-shaped) NGs.[12] Furthermore, curvature can also induce chirality into molecular nanographenes, thus showing chiroptical properties.[13] Actually, these domed molecular architectures have suitable geometries to host other chemical entities.[14] Concave-convex interactions between curved nanographenes and fullerenes are known to lead to supramolecular complexes with special interest as photoinduced electron transfer systems mimicking the photosynthetic process.[15] Additionally, the multi-electron acceptor nature of molecular NGs allows the reduction with alkali metals that normally remains hosted in the pockets of curved nanographenes leading to potential energy storage systems.[16]

In this work, we explore the chemical reduction of molecular NG **1**, previously synthesised in our research group,[17] with Na metal in THF (Scheme 1). The X-ray crystallography revealed the formation of a "naked" dianion $C_{76}H_{64}^{2-}$ ($\mathbf{1}^{2-}$) solvent-separated from the two cationic moieties {Na^+(18-crown-6)(THF)}. Additionally, in order to get a better understanding of this reduction process, changes in the electron density and aromaticity of **1** induced during the reduction process have been studied computationally by Density Functional Theory (DFT) calculations.

The chemical reduction of **1** was investigated with excess Na metal in anhydrous THF in the presence of 18-crown-6 at room temperature (Scheme 1). The reaction quickly proceeds to afford a dark brown solution (Figs. S1-S2, see ESI) which upon slow diffusion of hexanes produced dark brown blocks in good yield (see ESI for more details). The X-ray diffraction analysis confirmed the formation of a solvent-separated ion product (SSIP) with sodium counterions, [{Na^+(18-crown-6)(THF)}$_2$($\mathbf{1}^{2-}$)], which was crystallized with a half interstitial hexane molecule as **2**·0.5C_6H_{14} (see ESI for details).

In the crystal structure of **2** (Fig. 1), two cationic {Na^+(18-crown-6)(THF)} moieties are solvent-separated from the anionic

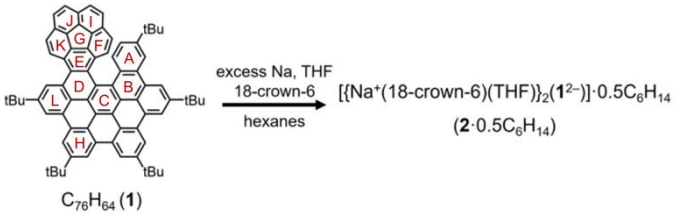

Scheme 1 Chemical reduction of $C_{76}H_{64}$ **1** with Na metal.

[a] *Department of Chemistry, University at Albany, State University of New York Albany, NY 12222, USA. E-mail: mpetrukhina@albany.edu*
[b] *School of Materials Science and Engineering, Tongji University, 4800 Cao'an Road, Shanghai 201804, China*
[c] *Departamento de Química Orgánica, Facultad de Ciencias Químicas, Universidad Complutense de Madrid, Ciudad Universitaria s/n 28040 Madrid, Spain. E-mail: israel@quim.ucm.es; nazmar@quim.ucm.es*
[d] *IMDEA-Nanociencia, C/Faraday, 9, Campus de Cantoblanco, 28049 Madrid, Spain.*
Electronic Supplementary Information (ESI) available: Details of preparation, X-ray diffraction, UV-vis, NMR, and calculation studies. CCDC 2142971–2142972. For ESI and crystallographic data in CIF or other electronic format see DOI: 10.1039/x0xx00000x.

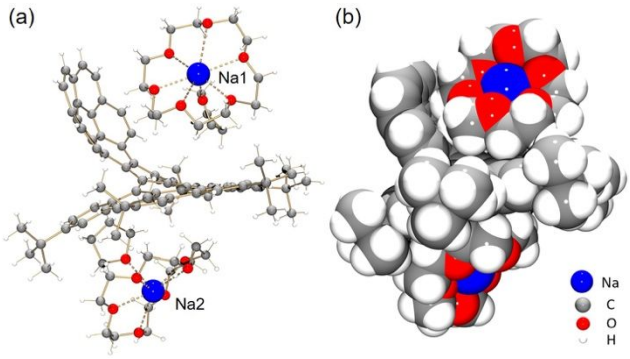

Fig. 1 Crystal structure of **2**, (a) ball-and-stick and (b) space-filling models.

core, providing the first example of a "naked" $\mathbf{1}^{2-}$ dianion. Each Na^+ ion is trapped by one 18-crown-6 ether and capped by one THF molecule, with the $Na–O_{crown}$ and $Na–O_{THF}$ distances of 2.462(13)–2.996(13) Å and 2.454(13)/2.473(13) Å, respectively. All Na–O distances are close to those reported in the literature.[16b,18] The coordination environment of Na^+ ions is completed by additional Na···O contacts with the adjacent 18-crown-6 ether molecule ($Na–O_{crown}$: 2.488(11) Å and 2.506(11) Å, respectively), thus forming dimeric cationic moieties which are commonly seen for light alkali metal ions like Na^+ and K^+.[16c,18a,19] Notably, compound **2** is racemic and contains an equimolar ratio of negatively-charged *P*- and *M*-isomeric molecular nanographenes. In the adjacent molecules (Fig. 2), two isomers of $\mathbf{1}^{2-}$ with opposite chirality form a cylindric internal space (1277 $Å^3$), which is capable of holding a $\{Na^+(18\text{-crown-6})(THF)\}_2$ dication (960 $Å^3$). The large internal cavity defined by the molecular curvature of the doubly-charged anions $\mathbf{1}^{2-}$ is similar to previously reported, where two less rigid nanographene units were used to entrap a C_{60} molecule.[17, 20]

In the solid-state structure of **2**, the $\{Na^+(18\text{-crown-6})(THF)\}_2$ dications are wrapped by two $\mathbf{1}^{2-}$ anions (C–H···π interactions: 2.417(3)–2.743(3) Å) (green lines in Fig. S11, see ESI). Those subunits are further linked into a 2D layer through C–H···π contacts between the convex surface of the corannulene bowl or of the hexabenzocoronene (HBC) core of the $\mathbf{1}^{2-}$ anions and the adjacent $\{Na^+(18\text{-crown-6})(THF)\}_2$ moieties (Fig. S12, see ESI) with the distances ranging over 2.679(3)–2.752(3) Å (purple lines in Fig. S11, see ESI). There are no significant interactions found between the adjacent layers in **2**.

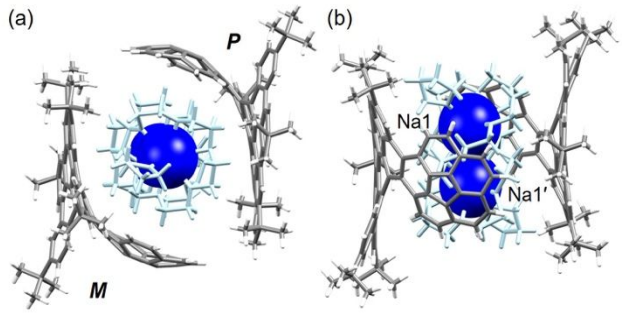

Fig. 2 (a) Top and (b) side views of two adjacent $\mathbf{1}^{2-}$ cores with opposite chirality wrapping a $\{Na^+(18\text{-crown-6})(THF)\}_2$ moiety in **2**, ball-and-stick models.

The deformation of this novel hybrid molecular nanographene upon two-electron uptake was analyzed using selected angles and bond length distances, revealing increasing distortion observed along the helicenic core. Before any comparison, the structure of neutral parent NG was recollected due to the low quality of the reported one.[17] The single crystals suitable for X-ray diffraction were grown by sublimation at 270 °C for 2 weeks. The space group is $P2_1/c$, and there is a half nitromethane molecule entrapped in the crystal that was squeezed out during structural refinement.

In order to describe the core distortion of the framework, the ring H has been selected as a reference plane. According to the dihedral angle calculation, in the neutral state, ∠A/H and ∠F/H are 12.2° and 48.2°, respectively, stemming from the intramolecular helical hindrance and the natural curvature of the bowl-shaped corannulene core in **1** (Table S2, see ESI). Upon two-electron addition, ∠A/F is dramatically increased to 80.8° (*vs.* 47.0° in **1**), showing the distortion of the helicenic core in $\mathbf{1}^{2-}$. Based on torsion angle calculation, the core deformation in **1** is spread through rings A–F (19.3°–27.7°) and enhanced near rings C and D in the doubly-charged anion (36.6° and 25.6° for torsion angles, and 714.4° and 712.0° for the sum of the interior angles, respectively) (Table S3, see ESI). Moreover, compared to the neutral state **1**, a notable elongation of most of the C–C bonds is observed (0.3 Å) in $\mathbf{1}^{2-}$, except for bonds C10–C11 and C12–C55 (Table S4, see ESI).

Besides, the structural deformation of the corannulene core in $\mathbf{1}^{2-}$ is clearly reflected by the C–C bond changes (Table S5, see ESI). The rim and spoke C–C bonds in $\mathbf{1}^{2-}$ are 1.385(3)–1.471(3) Å and 1.401(3)–1.420(3) Å, respectively, which are slightly elongated compared to neutral bowl. In contrast, the flank C–C bonds in $\mathbf{1}^{2-}$ are shortened (1.396(3)–1.477(3) Å), with all changes being analogous to those detected upon chemical reduction of corannulene.[18a,21] Notably, the bowl depth of the corannulene core in **1** (0.829(4) Å) is slightly deepened to 0.859(3) Å in its doubly-reduced form, which is consistent with the POAV calculations (Table S6, see ESI). This is opposite to the change of parent corannulene during chemical reduction (0.875(2) Å *vs.* 0.795(3) Å),[18a,21] but similar to that of the N-doped bowl (0.871(5) Å *vs.* 0.887(9) Å).[18b]

The addition of two electrons leads to the charge distribution change over the curved extended π-surface, as demonstrated by large downfield shifts of all aromatic signals in the ^{1}H NMR spectrum (Fig. 3). Moreover, it was also confirmed

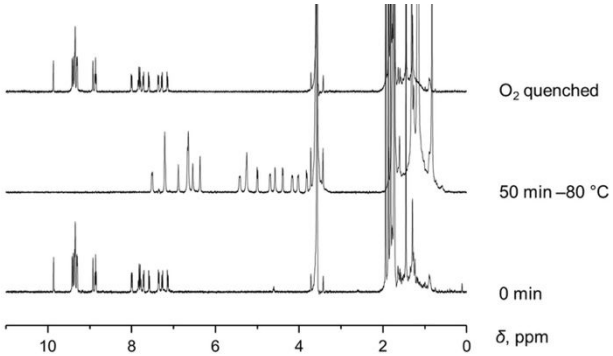

Fig. 3 ^{1}H NMR spectra of **1** (25 °C), *in situ* generated $\mathbf{1}^{2-}$ (–80 °C), and its quenched product (25 °C) in THF-d_8.

by NMR spectroscopy that the doubly-reduced $\mathbf{1}^{2-}$ anion can be reversibly re-oxidized back to the neutral state, which indicates the stability and inherent flexibility of helicenic core towards the redox process.

Results above clearly indicate that the electronic structure of the nanographene **1** is significantly modified upon the reduction process. To gain more insight into the $\mathbf{1}\rightarrow\mathbf{1}^{2-}$ transformation, DFT calculations were carried out at the dispersion corrected B3LYP-D3/def2-SVP level (see computational details in the ESI).

Fig. 4 shows that the LUMO of **1** is a π*-molecular orbital located mainly at the C=C double-bond fusing the corannulene and the PAH moieties (rings D/E in Table S2, see ESI). As a result, the first electron coming from the alkali metal upon reduction is essentially localized at these carbon atoms as confirmed by the computed spin density in the readily formed $\mathbf{1}^{-}$ radical anion (Fig. 4). Once the formation of the latter anion has occurred, a new reduction process takes place leading to the observed dianion $\mathbf{1}^{2-}$. Interestingly, simple visual inspection of the computed 3D molecular electrostatic potential (MEP) maps of the initial nanographene **1** and its reduced counterpart $\mathbf{1}^{2-}$ (Fig. 4) reveals that the introduced negative charges in the latter system are spread over the curved π-system, and particularly over the rings involved in the corannulene-PAH fusion and the adjacent rings, which is in line with the experimental observations (see above).

Our calculations therefore confirm that the stepwise reduction of nanographene **1** induces significant changes in its electronic structure. These changes should be also reflected in the aromaticity of the different rings of the nanographene and particularly, in the six-membered rings mostly affected by the reduction process, i.e., rings D/E (corannulene-PAH fusion) and adjacent rings (for a definition, see figure in Table S7, see ESI). To check this hypothesis, we compute the variation of the isotropic Nuclear Independent Chemical Shift (NICS)[22] values when going from $\mathbf{1}\rightarrow\mathbf{1}^{\bullet-}\rightarrow\mathbf{1}^{2-}$. From the data in Table S7 (see

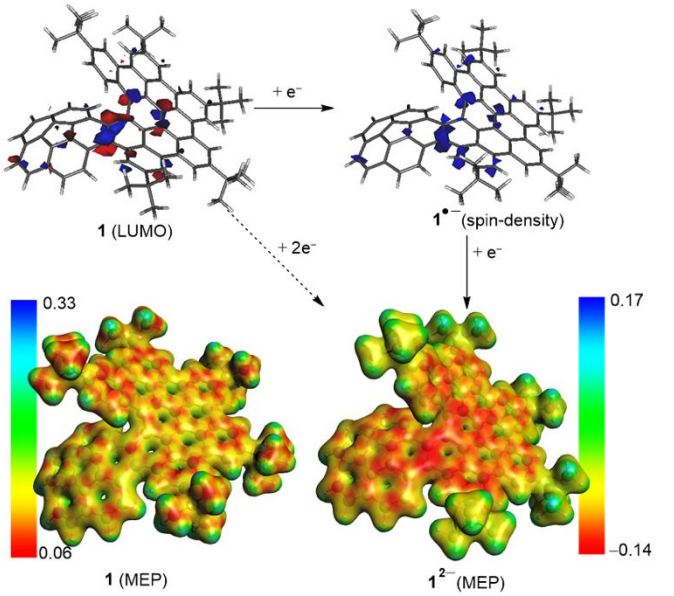

Fig. 4 Computed key species for the reduction of nanographene **1**. All data have been computed at the B3LYP-D3/def2-SVP level.

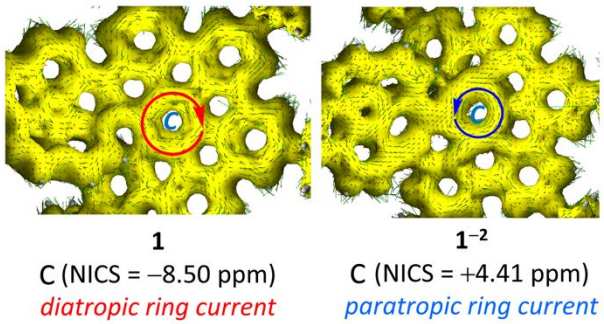

Fig. 5 Computed ACID plots for **1** and $\mathbf{1}^{2-}$ with a 0.04 au isosurface value.

ESI), it becomes evident that the reduction modifies the aromaticity strength of practically all the rings of the nanographene. Strikingly, the effect of the reduction on the aromaticity is much more pronounced in the rings involved in the fusion (D/E) as well as in the adjacent rings C, K and L. Indeed, whereas these key six-membered rings are aromatic or slightly aromatic in **1** (NICS values ranging from –0.43 to –8.50 ppm), they become non-aromatic or even antiaromatic in the reduced systems (NICS values ranging from +0.24 to +8.17 ppm). This noticeable aromaticity reversal confirms that the reduction of **1**, although affecting the electronic structure of the entire nanographene, takes place mainly at the corannulene-PAH fusion.

The above findings based on NICS calculations are supported by the Anisotropy of the Induced Current Density (ACID)[23] method. As shown in Fig. 5, the rings currents in **1** are clearly different for those in the reduced dianion $\mathbf{1}^{2-}$. For instance, for the key ring C, a clear diatropic (i.e., aromatic) ring current (clockwise vectors) is observed in **1** whereas a paratropic (i.e., antiaromatic) ring current (anticlockwise vectors) is computed for $\mathbf{1}^{2-}$. This aromaticity descriptor provides therefore further support to the above-commented aromaticity reversal upon reduction.

In summary, the chemical reduction of a corannulene-based chiral molecular nanographene **1** ($C_{76}H_{64}$) with Na metal afforded a new solvent-separated ion product which was characterized by single-crystal X-ray diffraction as [{Na^{+}(18-crown-6)(THF)}$_2$($\mathbf{1}^{2-}$)] (**2**). The addition of two electrons leads to a structural deformation of the whole hybrid molecular nanographene, as revealed by the enhanced distortion of the helicenic core and the bowl depth increase of corannulene in comparison to its neutral parent. Furthermore, the reduction process is fully reversible as proven by *in situ* NMR study. According to DFT calculations, the reduction occurs in a stepwise manner mainly at the C=C double bond fusing the corannulene and the PAH moieties of the nanographene. This reduction, although affecting the electron density of the entire system, provokes a remarkable aromaticity reversal (i.e., from weakly aromatic or aromatic to non-aromatic or antiaromatic) of the rings involved in the fusion as well as of the adjacent six-membered rings.

Conflicts of interest

There are no conflicts to declare.

Acknowledgements

Financial support of this work from the U. S. National Science Foundation, CHE-2003411, is acknowledged by M. A. P. NSF's ChemMatCARS Sector 15 is principally supported by the Divisions of Chemistry (CHE) and Materials Research (DMR), National Science Foundation, under grant number NSF/CHE-1834750. The use of the Advanced Photon Source, an Office of Science User Facility operated for the U.S. Department of Energy (DOE) Office of Science by Argonne National Laboratory, was supported by the U.S. DOE under Contract No. DE-AC02-06CH11357. Financial support from the Spanish MICINN (Projects PID2020-114653RB-I00 and RED2018-102815-T to N.M. and PID2019-106184GB-I00 and RED2018-102387-T to I.F.) is acknowledged.

Notes and references

1 (a) H. W. Kroto, J. R. Heath, S. C. O'Brien, R. F. Curl and R. E. Smalley, *Nature*, 1985, **318**, 162. (b) J. L. Delgado, S. Filippone, F. Giacalone, M. A. Herranz, B. Illescas, E. M. Pérez and N. Martín, *Top. Curr. Chem.*, 2014, **350**, 1.

2 (a) M. A. Petrukhina and L. T. Scott, *Fragments of Fullerenes and Carbon Nanotubes: Designed Synthesis, Unusual Reactions, and Coordination Chemistry*, John Wiley & Sons, Inc., Hoboken, NJ, 2012. (b) I. Fernández, *Chem. Sci*., 2020, **11**, 3769. (c) M. C. Stuparu, *Acc. Chem. Res*., 2021, **54**, 2858.

3 (a) L. T. Scott, M. M. Boorum, B. J. McMahon, S. Hagen, J. Mack, J. Blank, H. Wegner and A. de Meijere, *Science*, 2002, **295**, 1500. (b) M. Kabdulov, M. Jansen and K. Y. Amsharov, *Chem. Eur J*., 2013, **19**, 17262.

4 K. S. Novoselov, A. K. Geim, S. V. Morozov, D. Jiang, Y. Zhang, S. V. Dubonos, I. V. Grigorieva and A. A. Firsov, *Science*, 2004, **306**, 666.

5 (a) G. Bottari, M. A. Herranz, L. Wibmer, M. Volland, L. Rodríguez-Pérez, D. M. Guldi, A. Hirsch, N. Martín, F. D'Souza and T. Torres, *Chem. Soc. Rev*., 2017, **46**, 4464. (e) Z. X. Sun, S. Y. Fang and Y. H. Hu, *Chem. Rev.*, 2020, **120**, 10336.

6 (a) J. Wu, W. Pisula and K. Müllen, *Chem. Rev.,* 2007, **107**, 718. (b) N. Martín, *Adv. Energy Mater.,* 2017, **7**, 161102.

7 (a) M. Dvorak, W. Oswald and Z. G. Wu, *Sci. Rep.,* 2013, **3,** 2289. (b) T. Zhao, C. Xu, W. Ma, Z. B. Liu, T. Y. Zhou, Z. Liu, S. Feng, M. J. Zhu, N. Kang, D. M. Sun, H. M. Cheng and W. C. Ren, *Nat. Commun.,* 2019, **10**, 4854.

8 K. A. Ritter and J. W. Lyding, *Nat. Mater.*, 2009, **8**, 235. (b) Y. Morita, S. Suzuki, K. Sato and T. Takui, *Nat. Chem*., 2011, **3**, 197. (c) S.-Y. Li and L. He, *Front. Phys.*, 2022, **17**, 33201**.**

9 (a) A. Narita, X.-Y. Wang, X. Feng and K. Müllen, *Chem. Soc. Rev.*, 2015, **44**, 6616. (b) M. Stępień, E. Gonka, M. Zyla and N. Sprutta, *Chem. Rev.*, 2017, **117**, 3479.

10 (a) X. Li, M. Rui, J. Song, Z. Shen and H. Zeng, *Adv. Func. Mat*., 2015, **25**, 4929. (b) A. Ferrer-Ruiz, T. Scharl, P. Haines, L. Rodríguez-Pérez, A. Cadranel, M. A. Herranz, D. M. Guldi and N. Martin, *Angew. Chem. Int. Ed.*, 2018, **57**, 1001. (c) Y. Yan, J. Gong, J. Chen, Z. Zeng, W. Huang, K. Pu, J. Liu and P. Chen, *Adv. Mater*., 2019, **31**, e1808283. (d) A. Ferrer-Ruiz, T. Scharl, L. Rodríguez-Pérez, A. Cadranel, M. A. Herranz, N. Martín and D. M. Guldi, *J. Am. Chem. Soc.*, 2020, **142**, 20324.

11 (a) H. Ito, K. Ozaki and K. Itami, *Angew. Chem. Int. Ed.*, 2017, **56**, 11144. (b) M. Grzybowski, B. Sadowski, H. Butenschon and D. T. Gryko, *Angew. Chem. Int. Ed.*, 2020, **59**, 2998. (c) W. Matsuoka, H. Ito, D. Sarlah and K. Itami, *Nat. Commun.*, 2021, **12**, 3940.

12 (a) S. H. Pun and Q. Miao, *Acc. Chem. Res.*, 2018, **51**, 1630. (b) M. Rickhaus, M. Mayor and M. Juríček, *Chem. Soc. Rev*., 2017, **46**, 1643.

13 (a) J. M. Fernández-García, P. J. Evans, S. Filippone, M. A. Herranz and N. Martín, *Acc. Chem. Res*., 2019, **52**, 1565. (b) P. Izquierdo-García, J. M. Fernández-García, I. Fernández, J. Perles and N. Martín, J. *Am. Chem. Soc*., 2021, **143**, 11864. (c) J. M. Fernández-García, P.Izquierdo-García, M. Buendía, S. Filippone and N. Martín, *Chem. Commun*., 2022, DOI: 10.1039/D1CC06561K.

14 (a) M. Gallego, J. Calbo, J. Arago, R. M. K. Calderón, F. H. Liquido, T. Iwamoto, A. K. Greene, E. A. Jackson, E. M. Pérez, E. Ortí, D. M. Guldi, L. T. Scott and N. Martín, *Angew. Chem. Int. Ed.*, 2014, **53**, 2170. (c) J. I. Urgel, M. Di Giovannantonio, Y. Segawa, P. Ruffieux, L. T. Scott, C. A. Pignedoli, K. Itami and R. Fasel, *J. Am. Chem. Soc.*, 2019, **141**, 13158. (d) A. S. Filatov, M. V. Ferguson, S. N. Spisak, B. Li, C. F. Campana and M. A. Petrukhina, *Cryst. Growth Des.*, 2014, **14**, 756. (e) A. V. Zabula, Y. V. Sevryugina, S. N. Spisak, L. Kobryn, R. Sygula, A. Sygula and M. A. Petrukhina, *Chem. Commun.*, 2014, **50**, 2657.

15 (a) T. Kawase and H. Kurata, *Chem. Rev*., **2006**, 106, 5250. (b) M. Takeda, S. Hiroto, H. Yokoi, S. Lee, D. Kim and H. Shinokubo, *J. Am. Chem. Soc*., 2018, **140**, 6336. (c) X. Lu, T. Y. Gopalakrishna, Y. Han, Y. Ni, Y. Zou and J. Wu, *J. Am. Chem. Soc.*, 2019, **141**, 5934. (d) Q. Huang, G. Zhuang, H. Jia, M. Qian, S. Cui, S. Yang and P. Du, *Angew. Chem. Int. Ed*., 2019, **58**, 6244. (e) J. Urieta-Mora, M. Krug, W. Alex, J. Perles, I. Fernández, A. Molina-Ontoria, D. M. Guldi and N. Martín, *J. Am. Chem. Soc.,* 2020, **142**, 4162.

16 (a) Z. Zhou, S. N. Spisak, Q. Xu, A. Yu. Rogachev, Z. Wei, M. Marcaccio and M. A. Petrukhina, *Chem. Eur. J*., 2018, **24**, 3455. (b) Z. Zhou, X.-Y. Wang, Z. Wei, K. Müllen and M. A. Petrukhina, *Angew. Chem. Int. Ed.*, 2019, **58**, 14969. (c) Z. Zhou, L. Fu, Y. Hu, X.-Y. Wang, Z. Wei, A. Narita, K. Müllen and M. A. Petrukhina, *Angew. Chem. Int. Ed.*, 2020, **59**, 15923. (d) Y. Zhang, Y. Zhu, D. Lan, S. H. Pun, Z. Zhou, Z. Wei, Y. Wang, H. K. Lee, C. Lin, J. Wang, M. A. Petrukhina, Q. Li and Q. Miao, *J. Am. Chem. Soc*., 2021, **143**, 5231. (e) Z. Zhou, Z. Wei, K. Ikemoto, S. Sato, H. Isobe and M. A. Petrukhina, *Angew. Chem. Int. Ed.*, 2021, **60**, 11201. (f) S. N. Spisak, Z. Zhou, S. Liu, Q. Xu, Z. Wei, K. Kato, Y. Segawa, K. Itami, A. Yu. Rogachev and M. A. Petrukhina, *Angew. Chem. Int. Ed.*, 2021, **60**, 25445.

17 J. M. Fernández-García, P. J. Evans, S. Medina Rivero, I. Fernández, D. García-Fresnadillo, J. Perles, J. Casado and N. Martín, *J. Am. Chem. Soc.*, 2018, **140**, 17188.

18 (a) A. V. Zabula, S. N. Spisak, A. S. Filatov, V. M. Grigoryants and M. A. Petrukhina, *Chem. Eur. J.*, 2012, **18**, 6476. (b) Z. Zhou, Z. Wei, Y. Tokimaru, S. Ito, K. Nozaki and M. A. Petrukhina, *Angew. Chem. Int. Ed.*, 2019, **58**, 12107.

19 (a) Z. Zhou, R. K. Kawade, Z. Wei, F. Kuriakose, Ö. Üngör, M. Jo, M. Shatruk, R. Gershoni-Poranne, M. A. Petrukhina and I. V. Alabugin, *Angew. Chem. Int. Ed.*, 2020, **59**, 1256. (b) Z. Zhou, J. M. Fernández-García, Y. Zhu, P. J. Evans, R. Rodríguez, J. Crassous, Z. Wei, I. Fernández, M. A. Petrukhina and N. Martin, *Angew. Chem. Int. Ed.*, 2021, e202115747.

20 S. Zank, J. M. Fernández-García, A. Stasyuk, A. Vityuk, M. Krug, M. Solà, D. Guldi and N. Martín, *Angew. Chem. Int. Ed*., 2022, e202112834.

21 M. A. Petrukhina, K. W. Andreini, J. Mack and L. T. Scott, *J. Org. Chem.,* 2005, **70**, 5713.

22 Z. Chen, C. S. Wannere, C. Corminboeuf, R. Puchta and P. v. R. Schleyer, *Chem. Rev*., 2005, **105**, 3842.

23 (a) R. Herges and D. Geuenich, *J. Phys. Chem. A,* 2001, 105, 3214. (b) D. Geuenich, K. Hess, F. Köhler and R. Herges, *Chem. Rev*., 2005, **105**,3758.

